Bioorganic Chemistry 91 (2019) 103153

Contents lists available at ScienceDirect

Bioorganic Chemistry

journal homepage: www.elsevier.com/locate/bioorg

Synthesis, molecular docking analysis and carbonic anhydrase I-II inhibitory evaluation of new sulfonamide derivatives

Begüm Nurpelin Sağlık[a,b,*], Ulviye Acar Çevik[a,b], Derya Osmaniye[a,b], Serkan Levent[a,b], Betul Kaya Çavuşoğlu[a], Yeliz Demir[c], Sinem Ilgın[d], Yusuf Özkay[a,b], Ali Savaş Koparal[e], Şükrü Beydemir[f], Zafer Asım Kaplancıklı[a]

[a] Department of Pharmaceutical Chemistry, Faculty of Pharmacy, Anadolu University, 26470 Eskişehir, Turkey
[b] Doping and Narcotic Compounds Analysis Laboratory, Faculty of Pharmacy, Anadolu University, 26470 Eskişehir, Turkey
[c] Department of Pharmacy Services, Nihat Delibalta Göle Vocational High School, Ardahan University, 75700 Ardahan, Turkey
[d] Department of Toxicology, Faculty of Pharmacy, Anadolu University, 26470 Eskişehir, Turkey
[e] Open Education Faculty, Anadolu University, 26470 Eskişehir, Turkey
[f] Department of Biochemistry, Faculty of Pharmacy, Anadolu University, 26470 Eskişehir, Turkey

ARTICLE INFO

Keywords:
Carbonic anhydrase
Sulfonamide
Cytotoxicity
Molecular docking
ADME

ABSTRACT

New sulfonamide-hydrazone derivatives (**3a-3n**) were synthesized to evaluate their inhibitory effects on purified human carbonic anhydrase (hCA) I and II. The inhibition profiles of the synthesized compounds on hCA I-II isoenzyme were investigated by comparing their IC_{50} and K_i values. Acetazolamide (5-acetamido-1,3,4-thiadiazole-2-sulfonamide, AZA) has also been used as a standard inhibitor. The compound **3e** demonstrated the best hCA I inhibitory effect with a K_i value of 0.1676 ± 0.017 μM. Besides, the compound **3m** showed the best hCA II inhibitory effect with a K_i value of 0.2880 ± 0.080 μM. Cytotoxicity of the compounds **3e** and **3m** toward NIH/3T3 mouse embryonic fibroblast cell line was observed and the compounds were found to be non-cytotoxic. Molecular docking studies were performed to investigate the interaction types between active compounds and hCA enzymes. Pharmacokinetic profiles of compounds were assessed by theoretical ADME predictions. As a result of this study a novel and potent class of CA inhibitors were identified with a good activity potential.

1. Introduction

Carbonic anhydrases (CAs) are zinc enzymes strongly involved in regulating cell homeostasis, intracellular pH, fluid secretion, ion transport and biosynthetic reactions by catalyzing the reversible hydration of carbon dioxide (CO_2) to bicarbonate ion (HCO_3^-) and proton (H^+) [1–6]. CAs are common in almost all organisms, from simple to complex [7,8].

To date, fifteen isoforms (CA I to CA XV) of CA enzymes have been reported in humans. Among these isoforms, CA I-III, VII and XIII have been identified in cytosol, while CA IV, IX, XII and XIV have been defined as membrane bound enzymes. The subtypes of CA VA and CA VB are restricted to the mitochondrion, whereas CA VI is secreted in milk and saliva. These enzymes can be classified in terms of affinity to various inhibitors, subcellular localization, tissue distribution, and catalytic activity [9–13]. These processes include CA isoenzymes that serve as therapeutic targets prone to be inhibited to treat various disorders such as glaucoma, obesity, cancer, epilepsy, arthritis, neuropathic pain and osteoporosis [14–17]. CA I is found together with CA II in erythrocytes at high concentrations. CA II is the most active isoenzyme among CAs in human. hCA II is the most commonly found in the eye, kidney, central nervous system (CNS), and inner ear [18]. This enzyme is a target for drugs such as diuretics, antiglaucoma and anticonvulsants that are used clinically [19–22].

Sulfonamides ($R\text{-}SO_2NH_2$) represent an important class of chemicals possessing the potency to inhibit CA isoenzymes, which are involved in different pathological and physiological processes. These compounds bind to active site of CAs by an interaction between catalytic zinc ion of enzyme and deprotonated nitrogen of the sulfonamide moiety and block the CA enzymatic activity. Despite the supplementary interaction points offered from the sulfonamides within the CA, such a structural feature per se does not lead to selective isoenzyme binding. The CA isoenzyme selectivity of sulfonamide type CA inhibitors is related to molecular regions of compounds that are able to interact with hydrophobic and/or hydrophilic residues of the CA catalytic site [23–26].

Acetazolamide, dorzolamide, brinzolamide, methazolamide,

* Corresponding author at: Anadolu University, Faculty of Pharmacy, Department of Pharmaceutical Chemistry, 26470 Eskişehir, Turkey.
E-mail address: bnsaglik@anadolu.edu.tr (B.N. Sağlık).

https://doi.org/10.1016/j.bioorg.2019.103153
Received 26 December 2018; Received in revised form 23 May 2019; Accepted 24 July 2019
Available online 29 July 2019
0045-2068/

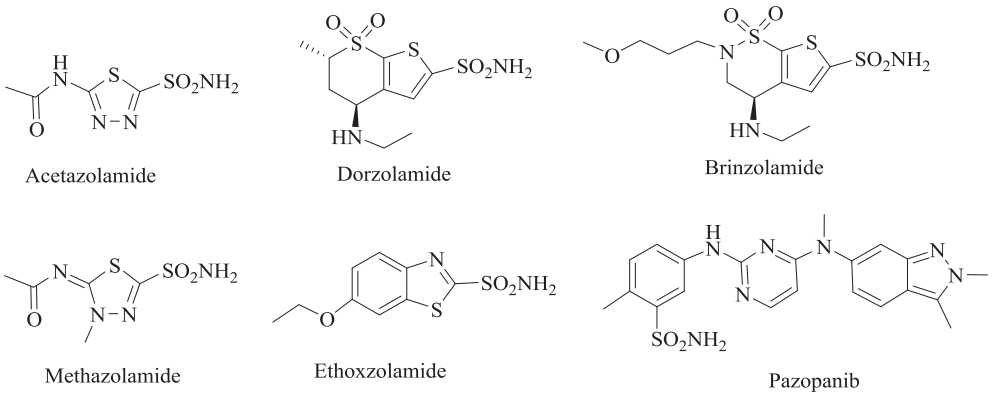

Fig. 1. Chemical structures of some carbonic anhydrase inhibitors which are in clinical use.

ethoxzolamide, and pazopanib are clinically important CA inhibitors that carry sulfonamide pharmacophore (Fig. 1). CA inhibitors have *in vitro* selectivity differences against the 13 active isozymes, however none of them is convincingly selective in vivo or clinically [27]. Thus, there common side effects including taste alterations, depression, weight loss, blurred vision, burning of the eye, and kidney stones for non-spesific CA inhibitors [28–31]. This situation reveals that there is a need to enhance the selectivity and inhibition potency of CA inhibitors towards isoenzymes

Hydrazones, characterized by the presence of a open chain −CO−NH−N=CH-group, are used as building blocks for the synthesis of a variety of useful bioactive compounds due to their flexibility and structural similarities to various natural substances of biological importance. The extensive pharmacological activity of hydrazone analogs has led to considerable research. [32–35]. Moreover, several examples of compounds including hydrazone moiety have been reported as CA inhibitors [36–38].

Based on the above information, we focused on the synthesis of compounds that carry the hydrazone and sulfonamide pharmacophores in the same chemical structure and investigated their inhibitor effects on hCA I and II isoenzymes.

2. Experimental

2.1. Chemistry

Chemicals used in the synthesis were purchased from Sigma-Aldrich (Sigma-Aldrich Corp., St. Louis, MO, USA) or Merck (Merck KGaA, Darmstadt, Germany) chemical companies and were used without further chemical purifications. Melting points (MP) were determined by an automatic melting point apparatus (MP90, Mettler-Toledo, OH, USA). The NMR spectra (^{1}H and ^{13}C) were recorded in DMSO-d_6 by a Bruker digital FT-NMR spectrometer (Bruker Bioscience, MA, USA) at 300 MHz and 75 MHz, respectively. The IR spectra were recorded by an IRAffinity-1S Fourier transform IR (FTIR) spectrometer (Shimadzu, Tokyo, Japan). HRMS studies were performed on an LCMS-IT-TOF system (Shimadzu, Tokyo, Japan). Chemical purities of the compounds were checked by classical TLC applications performed on silica gel 60 F_{254} (Merck KGaA, Darmstadt, Germany).

2.1.1. 2-Chloro-N-(4-sulfamoylphenyl)acetamide (1)

Chloroacetyl chloride (2.16 mL, 27.8 mmol) was added dropwise with stirring to a solution of 4-aminobenzenesulfonamide (4 g, 23.2 mmol) in DMF (20 mL). After the completion of dropping, the mixture was stirred for 1 h and then poured into the iced-water (100 mL). Precipitated product was filtered, washed with water, dried, and recrystallized from ethanol.

2.1.2. 2-Hydrazinyl-N-(4-sulfamoylphenyl)acetamide (2)

Excess of hydrazine hydrate (5 mL) was added in portions into a solution of 2-chloro-N-(4-sulfamoylphenyl)acetamide (**1**) (5.19 g, 20.9 mmol) in EtOH. The reaction mixture was stirred for 15 h at room temperature. The precipitated product was filtered and washed with cold EtOH to remove the excess of the hydrazine hydrate. Raw product was dried, and recrystallized from EtOH.

2.1.3. General procedure for the synthesis of target compounds (3a-3n)

A mixture of 2-hydrazinyl-N-(4-sulfamoylphenyl)acetamide (**2**) (0.3 g, 1.24 mmol), appropriate aromatic benzaldehydes (1.24 mmol) and catalytic quantity of acetic acid was refluxed in EtOH for 2 h. The mixture was cooled down in an ice-bath, precipitated product was filtered, dried and recrystallized from EtOH.

*2.1.3.1. N-(4-Sulfamoylphenyl)-2-(2-(thiophen-2-ylmethylene)hydrazinyl) acetamide **(3a)***. Yield: 81%, M.P. = 163–164 °C, FTIR (ATR, cm^{-1}): 3313 (N−H), 1707 (C=O), 1155 (C−N), 825. ^{1}H NMR (300 MHz, DMSO-d_6): δ = 3.92 (2H, d, J = 5.30 Hz, −CH_2), 7.00 (1H, dd, J = 5.04–3.60 Hz, Thiophene CH), 7.09 (1H, d, J = 3.60 Hz, Thiophene CH), 7.24 (2H, s, −NH_2), 7.36 (1H, d, J = 5.04 Hz, Thiophene CH), 7.53 (1H, t, J = 5.30 Hz, −NH), 7.76 (2H, s, Disubstituted Benzene −CH), 7.77 (2H, s, Disubstituted Benzene −CH), 7.90 (1H,s, −CH=N), 10.27 (1H, s, −NH) ^{13}C NMR (75 MHz, DMSO-d_6): δ = 52.67, 119.24, 125.53, 126.27, 127.17, 127.81, 132.36, 138.90, 141.77, 142.16, 169.99. HRMS (m/z): $[M + H]^+$ calcd for $C_{15}H_{13}N_3O_2S_3$: 364.0243; found: 364.0249.

*2.1.3.2. 2-(2-((3-Methylthiophen-2-yl)methylene)hydrazinyl)-N-(4-sulfamoylphenyl)acetamide **(3b)***. Yield: 75%, M.P. = 150–151 °C, FTIR (ATR, cm^{-1}): 3329 (N−H), 1697 (C=O), 1151 (C−N), 827. ^{1}H NMR (300 MHz, DMSO-d_6): δ = 2.40 (3H, s, CH_3), 4.17 (2H, d, J = 4.17 Hz, −CH_2), 6.91 (1H, d, J = 3.63 Hz, Thiophene CH), 7.25 (2H, s, −NH_2), 7.39 (1H, d, J = 3.60 Hz, Thiophene CH), 7.41 (1H, t, J = 5.25 Hz, −NH), 7.77 (4H, s, Disubstituted Benzene −CH), 7.88 (1H, s, −CH=N), 10.43 (1H, s, −NH). ^{13}C NMR (75 MHz, DMSO-d_6): δ = 14.19, 51.16, 119.38, 125.63, 127.23, 130.38, 131.77, 138.35, 139.06, 142.05, 142.53, 168.29. HRMS (m/z): $[M + H]^+$ calcd for $C_{16}H_{15}N_3O_2S_3$: 378.0399; found: 378.0390.

*2.1.3.3. 2-(2-((5-Methylthiophen-2-yl)methylene)hydrazinyl)-N-(4-sulfamoylphenyl)acetamide **(3c)***. Yield: 78%, M.P. = 163–164 °C. FTIR (ATR, cm^{-1}): 3327 (N−H), 1703 (C=O), 1151 (C−N). ^{1}H NMR (300 MHz, DMSO-d_6): δ = 2.38 (3H, s, −CH_3), 3.92 (2H, d, J = 5.25 Hz, −CH_2), 6.69 (1H, d, J = 3.48 Hz, Thiophene CH), 6.88 (1H, d, J = 3.48 Hz, Thiophene CH), 7.25 (2H, s, −NH_2), 7.41 (1H, t, J = 5.25 Hz, −NH), 7.77 (2H, s, Disubstituted Benzene −CH), 7.78 (2H, s, Disubstituted Benzene −CH), 7.89 (1H,s, −CH=N), 10.26 (1H, s, −NH). ^{13}C NMR (75 MHz, DMSO-d_6): δ = 15.64, 52.78, 119.22,

126.04, 126.47, 127.16, 127.24, 133.01, 138.89, 142.05, 142.16, 168.29. HRMS (*m/z*): $[M + H]^+$ calcd for $C_{16}H_{15}N_3O_2S_3$: 377.0399; found: 377.0392.

2.1.3.4. 2-(2-((5-Bromothiophen-2-yl)methylene)hydrazinyl)-N-(4-sulfamoylphenyl)acetamide ***(3d)***. Yield: 84%, M.P. = 188–189 °C, FTIR (ATR, cm^{-1}): 3336 (N—H), 1681 (C═O), 1155 (C—N), 825. ^{1}H NMR (300 MHz, DMSO-d_6): δ 3.96 (2H, d, J = 5.10 Hz, $-CH_2$), 6.91 (1H, d, J = 3.84 Hz, Thiophene CH), 7.10 (1H, d, J = 3.81 Hz, Thiophene CH), 7.24 (2H, s, $-NH_2$), 7.74 (1H, t, J = 5.67 Hz, —NH), 7.76 (4H, br. s, Disubstituted Benzene —CH), 7.78 (1H,s, —CH═N), 10.28 (1H, s, —NH) ^{13}C NMR (75 MHz, DMSO-d_6): δ = 52.38, 110.67, 119.25, 126.33, 127.17, 130.90, 131.14, 138.92, 142.14, 143.93, 169.66. HRMS (*m/z*): $[M + H]^+$ calcd for $C_{15}H_{12}N_3O_2S_3Br$: 441.9348; found: 440.9343.

2.1.3.5. 2-(2-((5-Nitrothiophen-2-yl)methylene)hydrazinyl)-N-(4-sulfamoylphenyl)acetamide ***(3e)***. Yield: 92%, M.P. = 177–178 °C, FTIR (ATR, cm^{-1}): 3329 (N—H), 1695 (C═O), 1151 (C—N), 829. ^{1}H NMR (300 MHz, DMSO-d_6): δ 4.13 (2H, d, J = 5.10 Hz, $-CH_2$), 7.12 (1H, d, J = 4.44 Hz, Thiophene CH), 7.25 (2H, s, $-NH_2$), 7.75 (1H, s, —CH═N), 7.77 (4H, br. s, Disubstituted Benzene —CH), 8.00 (1H, d, J = 4.41 Hz, Thiophene CH), 8.68 (1H, t, J = 4.90 Hz, —NH), 10.39 (1H, s, —NH) ^{13}C NMR (75 MHz, DMSO-d_6): δ = 51.82, 119.30, 124.34, 127.16, 127.20, 131.66, 139.01, 142.08, 147.62, 151.66, 168.64. HRMS (*m/z*): $[M + H]^+$ calcd for $C_{15}H_{12}N_4O_4S_3$: 409.0093; found: 408.0087.

2.1.3.6. 2-(2-((1H-pyrrol-2-yl)methylene)hydrazinyl)-N-(4-sulfamoylphenyl)acetamide ***(3f)***. Yield: 76%, M.P. = oil, FTIR (ATR, cm^{-1}): 3257 (N—H), 1693 (C═O), 1149 (C—N), 831. ^{1}H NMR (300 MHz, DMSO-d_6): δ 4.08 (2H, d, J = 5.00 Hz, $-CH_2$), 6.22 (1H, m, Pyrrole —CH), 6.64 (1H, m, Pyrrole —CH), 7.08 (1H, m, Pyrrole —CH), 7.25 (2H, s, $-NH_2$), 7.76 (1H, s, —CH═N), 7.77 (2H, s, Disubstituted Benzene —CH), 7.78 (2H, s, Disubstituted Benzene —CH), 8.08 (1H, t, J = 4.90 Hz, —NH), 10.41 (1H, s, —NH), 11.17 (1H, s, pyrrole —NH) ^{13}C NMR (75 MHz, DMSO-d_6): δ = 51.63, 104.67, 115.16, 119.72, 124.47, 126.38, 127.81, 133.94, 139.21, 142.42, 168.64. HRMS (*m/z*): $[M + H]^+$ calcd for $C_{15}H_{14}N_4O_2S_2$: 347.0631; found: 347.0623.

2.1.3.7. 2-(2-((1-Methyl-1H-pyrrol-2-yl)methylene)hydrazinyl)-N-(4-sulfamoylphenyl)acetamide ***(3g)***. Yield: 77%, M.P. = oil, FTIR (ATR, cm^{-1}): 3246 (N—H), 1660 (C═O), 1151 (C—N), 829. ^{1}H NMR (300 MHz, DMSO-d_6): δ 3.81 (3H, s, $-OCH_3$), 3.87 (3H, s, $-CH_3$), 4.59 (2H, d, J = 4.17 Hz, $-CH_2$), 6.09 (1H, dd, J = 3.75–2.61 Hz, Pyrrole CH), 6.47 (1H, dd, J = 3.78–1.74 Hz, Pyrrole CH), 6.95–6.96 (1H, m, Pyrrole CH), 7.26 (2H, s, $-NH_2$), 7.76 (1H, s, —CH═N), 7.77 (2H, s, Disubstituted Benzene —CH), 7.78 (2H, s, Disubstituted Benzene —CH), 8.08 (1H, t, J = 4.90 Hz, —NH), 10.39 (1H, s, —NH). ^{13}C NMR (75 MHz, DMSO-d_6): δ = 35.74, 51.68, 104.71, 115.43, 119.72, 124.85, 126.38, 127.81, 133.94, 139.21, 142.42, 168.64. HRMS (*m/z*): $[M + H]^+$ calcd for $C_{16}H_{16}N_4O_2S_2$: 361.0787; found: 361.0779.

2.1.3.8. 2-(2-(Furan-2-ylmethylene)hydrazinyl)-N-(4-sulfamoylphenyl) acetamide ***(3h)***. Yield: 79%, M.P. = 146–147 °C, FTIR (ATR, cm^{-1}): 3267 (N—H), 1681 (C═O), 1151 (C—N). ^{1}H NMR (300 MHz, DMSO-d_6): δ 4.62 (2H, d, J = 4.32 Hz, $-CH_2$), 6.61–6.64 (1H, m, Furan CH), 6.92 (1H d, J = 3.42 Hz, Furan CH), 7.26 (2H, s, $-NH_2$), 7.76 (1H, s, —CH═N), 7.77 (2H, s, Disubstituted Benzene —CH), 7.78 (2H, s, Disubstituted Benzene —CH), 7.82–7.83 (1H, m, Furan CH), 7.95 (1H, t, J = 4.50 Hz, —NH), 10.46 (1H, s, —NH). ^{13}C NMR (75 MHz, DMSO-d_6): δ = 51.99, 112.65, 114.43, 119.72, 127.81, 133.94, 139.21, 142.42, 143.86, 149.19, 168.10. HRMS (*m/z*): $[M + H]^+$ calcd for $C_{15}H_{13}N_3O_3S_2$: 348.0471; found: 348.0466.

2.1.3.9. 2-(2-((5-Methylfuran-2-yl)methylene)hydrazinyl)-N-(4-sulfamoylphenyl)acetamide ***(3i)***. Yield: 79%, M.P. = 145–146 °C, FTIR (ATR, cm^{-1}): 3246 (N—H), 1701 (C═O), 1151 (C—N), 790.^{1}H NMR (300 MHz, DMSO-d_6): δ 2.34 (3H, s, $-CH_3$), 4.61 (2H, d, J = 4.32 Hz, $-CH_2$), 6.25–6.26 (1H, m, Furan CH), 6.80 (1H d, J = 3.24 Hz, Furan CH), 7.26 (2H, s, $-NH_2$), 7.76 (1H, s, —CH═N), 7.77 (2H, s, Disubstituted Benzene —CH), 7.78 (2H, s, Disubstituted Benzene —CH), 7.95 (1H, t, J = 4.50 Hz, —NH), 10.46 (1H, s, —NH). ^{13}C NMR (75 MHz, DMSO-d_6): δ = 14.01, 52.06, 105.00, 109.07, 114.19, 119.15, 127.68, 134.68, 137.33, 147.92, 155.10, 168.23. HRMS (*m/z*): $[M + H]^+$ calcd for $C_{16}H_{15}N_3O_3S_2$: 362.0628; found: 362.0632.

2.1.3.10. 2-(2-((5-nitrofuran-2-yl)methylene)hydrazinyl)-N-(4-sulfamoylphenyl)acetamide ***(3j)***. Yield: 80%, M.P. = 169–170 °C, FTIR (ATR, cm^{-1}): 3334 (N—H), 1701 (C═O), 1149 (C—N), 833. ^{1}H NMR (300 MHz, DMSO-d_6): δ 4.17 (2H, d, J = 4.41 Hz, $-CH_2$), 6.79 (1H, d, J = 3.99 Hz, Furan CH), 7.25 (2H, s, $-NH_2$), 7.52 (1H, s, —CH═N), 7.71 (1H, d, J = 3.96 Hz, Furan CH), 7.77 (4H, br. s, Disubstituted Benzene —CH), 8.80 (1H, t, J = 4.44 Hz, —NH), 10.41 (1H, s, —NH) ^{13}C NMR (75 MHz, DMSO-d_6): δ = 51.89, 109.88, 116.51, 119.27, 121.78, 127.22, 139.01, 142.07, 150.99, 155.77, 168.77. HRMS (*m/z*): $[M + H]^+$ calcd for $C_{15}H_{12}N_4O_5S_2$: 393.0322; found: 393.0315.

2.1.3.11. 2-(2-((1H-imidazol-2-yl)methylene)hydrazinyl)-N-(4-sulfamoylphenyl)acetamide ***(3k)***. Yield: 82%, M.P. = 178–179 °C, FTIR (ATR, cm^{-1}): 3344 (N—H), 1695 (C═O), 1155 (C—N), 839. ^{1}H NMR (300 MHz, DMSO-d_6): δ 4.69 (2H, d, J = 4.32 Hz, $-CH_2$-), 6.67 (2H, s, Imidazole —CH), 7.26 (2H, s, $-NH_2$), 7.51 (2H, s, Imidazole —NH), 7.72 (1H, s, —CH═N), 7.77 (2H, s, Disubstituted Benzene —CH), 7.78 (2H, s, Disubstituted Benzene —CH), 7.82–7.83 (1H, m, Furan CH), 7.95 (1H, t, J = 4.50 Hz, —NH), 10.49 (1H, s, —NH). ^{13}C NMR (75 MHz, DMSO-d_6): δ = 51.98, 119.25, 121.54, 126.73, 130.37, 133.94, 141.56, 144.02, 168.97. HRMS (*m/z*): $[M + H]^+$ calcd for $C_{16}H_{14}N_4O_2S_2$: 359.0631; found: 359.0635.

2.1.3.12. 2-(2-((1-Methyl-1H-imidazol-2-yl)methylene)hydrazinyl)-N-(4-sulfamoylphenyl)acetamide ***(3l)***. Yield: 82%, M.P. = 160–161 °C, FTIR (ATR, cm^{-1}): 3342 (N—H), 1687 (C═O), 1153 (C—N), 839. ^{1}H NMR (300 MHz, DMSO-d_6): δ 4.17 (2H, d, J = 4.38 Hz, $-CH_2$), 6.81 (1H, s, Imidazole —CH), 7.09 (1H, s, Imidazole —CH), 7.25 (2H, s, $-NH_2$), 7.65 (1H, s, —CH═N), 7.77 (4H, br. s, Disubstituted Benzene —CH), 8.80 (1H, t, J = 4.44 Hz, —NH), 10.36 (1H, s, —NH) ^{13}C NMR (75 MHz, DMSO-d_6): δ = 13.82, 51.89, 119.27, 121.16, 126.83, 127.22, 139.01, 142.07, 144.42, 149.82, 168.77. HRMS (*m/z*): $[M + H]^+$ calcd for $C_{16}H_{14}N_4O_2S_2$: 359.0631; found: 359.0628.

2.1.3.13. 2-(2-(Pyridin-3-ylmethylene)hydrazinyl)-N-(4-sulfamoylphenyl) acetamide ***(3m)***. Yield: 82%, M.P. = 162–163 °C, FTIR (ATR, cm^{-1}): 3350 (N—H), 1689 (C═O), 1151 (C—N), 896. ^{1}H NMR (300 MHz, DMSO-d_6): δ 4.10 (2H, d, J = 4.11 Hz, $-CH_2$), 7.25 (2H, s, $-NH_2$), 7.42 (1H, m, Pyridine CH), 7.59 (1H, s, —CH═N), 7.76 (2H, br. s, Disubstituted Benzene —CH), 7.78 (2H, br. s, Disubstituted Benzene —CH), 8.13 (1H, m Pyridine CH), 8.23 (1H, t, J = 4.08 Hz, —NH), 8.78 (2H, m Pyridine CH), 10.39 (1H, s, —NH). ^{13}C NMR (75 MHz, DMSO-d_6): δ = 52.03, 119.24, 122.15, 127.14, 130.83, 131.72, 134.13, 138.90, 143.72, 148.02, 149.65, 168.11. HRMS (*m/z*): $[M + H]^+$ calcd for $C_{16}H_{14}N_4O_2S_2$: 359.0631; found: 359.0628.

2.1.3.14. 2-(2-(Pyridin-4-ylmethylene)hydrazinyl)-N-(4-sulfamoylphenyl) acetamide ***(3n)***. Yield: 82%, M.P. = 157–158 °C, FTIR (ATR, cm^{-1}): 3350 (N—H), 1700 (C═O), 1151 (C—N), 840. ^{1}H NMR (300 MHz, DMSO-d_6): δ 4.10 (2H, d, J = 4.08 Hz, $-CH_2$), 7.25 (2H, s, $-NH_2$), 7.40 (2H, d, J = 6.12 Hz, Pyridine CH), 7.57 (1H, s, —CH═N), 7.76 (2H, br. s, Disubstituted Benzene —CH), 7.78 (2H, br. s, Disubstituted Benzene —CH), 8.29 (1H, t, J = 4.08 Hz, —NH), 8.45 (2H, d, J = 6.09 Hz, Pyridine CH), 10.53 (1H, s, —NH). ^{13}C NMR (75 MHz, DMSO-d_6): δ = 52.19, 119.24, 122.96, 127.14, 131.99, 138.90, 142.22, 143.91,

150.23, 169.47. HRMS (*m/z*): $[M + H]^+$ calcd for $C_{16}H_{14}N_4O_2S_2$: 359.0631; found: 359.0628.

2.2. Biological activity

2.2.1. Purification of CA isozymes from human erythrocytes by affinity chromatography

Erythrocytes were purified from fresh human blood obtained from the Blood Center, Atatürk University. The blood samples were centrifuged to separate erythrocytes at 1500 rpm for 15 min and plasma and buffy coat were carefully removed. Then, underlying erythrocytes washed twice with 0.9% NaCl and hemolysed with 1.5 volumes of ice-cold water. It was stirred for half an hour at 4 °C. The hemolysate was centrifuged at 20,000 rpm for 30 min at 4 °C and cell membranes were separated. pH was adjusted to 8.7 with solid Tris. The hemolysate was applied to the prepared Sepharose 4B-L-tyrosine-sulfanylamide affinity column equilibrated with 25 mM Tris-HCl/0.1 M Na_2SO_4 (pH 8.7). The affinity gel was washed with 25 mM Tris-HCl/22 mM Na_2SO_4 (pH 8.7). The human CA isozymes (hCA-I and hCA-II) were eluted with 1 M NaCl/25 mM Na_2HPO_4 (pH 6.3) and 0.1 M $NaCH_3COO$/0.5 M $NaClO_4$ (pH 5.6), respectively. All procedures were performed at 4 °C [39].

2.2.2. Measurement of CA activity

2.2.2.1. Hydratase activity assay. CA activity was determined using the Wilbur-Anderson Method [40]. This method, as a result hydration of CO_2 is released H^+ ions and the pH changes were determined by means of bromine thymol blue indicator, based on measuring the elapsed time. CO_2–Hydratase activity as an enzyme unit (EU) was calculated by using the equation (to-tc/tc) where to and tc are the times for pH change of the nonenzymatic and the enzymatic reactions, respectively.

2.2.2.2. Esterase activity assay. Esterase activity of human erythrocyte CA was assayed by following the change in absorbance at 348 nm of 4-nitrophenyl acetate to 4-nitrophenolate ion over a period of 3 min at 25 °C using a spectrophotometer according to the method described by Verpoorte et al. [41].

2.2.3. Inhibition assays

The inhibitory effects of newly synthesized compounds on CA enzyme activity were tested in triplicate at each concentration used. IC_{50} values were calculated for the compounds at different concentrations by utilizing graphs of activity %. The activities of enzymes in the medium without inhibitors were used as 100% activity. The K_i values of the compounds were calculated by Lineweaver-Burk graphics.

2.3. Cytotoxicity test

NIH/3T3 mouse embryonic fibroblast cell line (ATCC CRL 1658) was used for cytotoxicity study. Cells were replicated into Dulbecco's Modified Eagle's Medium (DMEM) containing 10% fetal bovine serum (FBS), 1% 100 IU/mL penicillin/100 mg/mL streptomycin, at 37 °C in a humidified atmosphere of 95% air and 5% CO_2. The proliferation of the NIH/3T3 cell line was assessed by MTT (3-(4,5-Dimethylthiazol-2-yl)-2,5-Diphenyltetrazolium bromide) assay. Briefly, cells were inoculated into 96-well culture plates at densities of 10,000 cells per well. After 24 h, they were treated with synthesized compounds (concentrations of 200–0.39 μg/mL) for 24 h. After the incubation period, MTT solution (5 mg/mL) was added to each well and incubated for 3 h at 37 °C. At the end of the incubation, the purple MTT-formazan crystals were dissolved by adding 100 μg/ml of DMSO to each well. The plates were then read on a Microplate reader at 540 nm wavelength [42,43]. The IC_{50} value was calculated from the plots of cell proliferations against concentrations by applying regression analyses on GraphPad Prism Version 5.

2.4. Prediction of ADME parameters

Physicochemical parameters of synthesized compounds (**3a-3n**) were calculated by using *QikProp 4.8*. [44].

2.5. Molecular docking studies

A Docking study was performed to seek binding modes of compounds **3e** and **3m** to CA I and CA II enzyme active sites, respectively. The crystal structures of CA I (PDB ID: 1AZM) [45] and CA II (PDB ID: 3HS4) [46] were retrieved from the Protein Data Bank server (www.pdb.org).

The chemical structures of ligands were drawn using the *Schrödinger Maestro* [47] interface and then were submitted to the *Protein Preparation Wizard* protocol of the *Schrödinger Suite 2016 Update 2* [48]. Then the ligands were prepared by the *LigPrep 3.8* [49] to set to protonation states at pH 7.4 ± 1.0 and the atom types, correctly. Bond orders were assigned, and hydrogen atoms were added to the structures. The grid generation was formed using *Glide 7.1* [50]. Flexible docking runs were performed with single precision docking mode (SP).

3. Results and discussion

3.1. Chemistry

The compounds **3a-3n** were synthesized as summarized as Scheme 1. Initially, 2-Chloro-N-(4-sulfamoylphenyl)acetamide (**1**) was prepared by means of the acetylation reaction using chloroacetyl chloride. In the second step, 2-Chloro-N-(4-sulfamoylphenyl)acetamide (**1**) and excess of hydrazine hydrate were stirred at room temperature to obtain 2-hydrazinyl-N-(4-sulfamoylphenyl)acetamide (**2**). Finally, compound **2** and appropriate aromatic benzaldehydes were reacted to gain the compounds **3a-3n**.

Structure of the synthesized were elucidated by IR, ^{1}H NMR, ^{13}C NMR and mass spectroscopic analyses. In the IR spectroscopy, N—H bond of hydrazide was observed over 3246 cm^{-1}. Carbonyl group (C═O) had a band about 1681–1707 cm^{-1}. In ^{1}H NMR spectrum, methoxy (—OCH_2) protons and methylene (—CH_2-) protons between sulphur atom and carbonyl group gave singlet peaks at 3.81–3.82 ppm and between 4.55 and 4.70 ppm, respectively. Benzimidazole H_5 gave a doublet of doublet peak at 6.99 ppm with coupling constants values 8.8 Hz and 2.5 Hz. Benzimidazole H_4 and H_6 protons were observed between 7.37 and 7.42 ppm and 7.86–7.87 ppm, respectively. Methine (—CH═) proton of hydrazide group recorded as a singlet peak between 7.87 and 8.29 ppm, depending on the electronic nature of substituents. Proton of hydrazone nitrogen (—CONHN═) had a singlet peak over 11.39 ppm. The aromatic peaks of variable heterocyclic rings were observed between 6.09 and 8.88 ppm. In ^{13}C NMR spectrum, aliphatic carbons were recorded between 14.01 and 56.01 ppm, while aromatic carbons were observed between 104.96 and 169.23 ppm. In the HRMS, all masses were matched well with the expected M + H values.

3.2. Biological activity

The newly prepared sulfonamides **3a-3n** were evaluated for their ability to inhibit two physiologically relevant hCA isoforms, hCA I and II. The inhibition data (IC_{50} and K_i) of the prepared compounds and the standard inhibitor acetazolamide (AZA) against hCA isoforms are summarized in Table 1.

The IC_{50} values of compounds against hCA I were calculated between 0.176 μM and 2.398 μM, whereas IC_{50} values against hCA II were in the range of 0.526 μM to 2.484 μM. The compounds **3e** and **3m** showed notable inhibitory effects against hCA I and hCA II, respectively. Compound **3e** (IC_{50} = 0.176 μM) showed the strongest and selective inhibition toward hCA I enzyme, while **3m** was found to be the most active (IC_{50} = 0.526 μM) and selective derivative against hCA II.

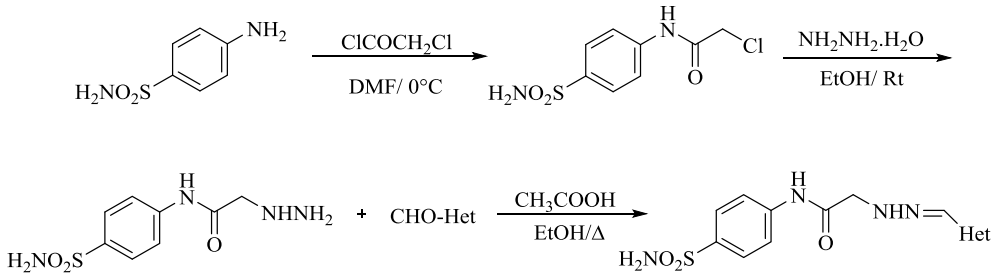

Comp.	Het
3a	Thiophen-2-yl
3b	3-Methylthiophen-2-yl
3c	5-Methylthiopen -2-yl
3d	5-Bromothiophen-2-yl
3e	5-Nitrothiophen-2-yl
3f	*1H*-pyrrol-2-yl
3g	1-Methyl-*1H*-pyrrol-2-yl
3h	Furan-2-yl
3i	5-Methylfuran-2-yl
3j	5-Nitrofuran-2-yl
3k	*1H*-imidazol-2-yl
3l	1-Methyl-*1H*-imidazol-2-yl
3m	Pyridin-3-yl
3n	Pyridin-4-yl

Scheme 1. Synthesis of target compounds.

Table 1 gives some important information about structure activity relationships. Compounds **3e** (IC_{50} = 0.176 μM) and **3j** (IC_{50} = 0.264 μM), bearing 5-nitrothiophene and 5-nitrofuran substructures, have higher inhibition potency against hCA I when compared with other derivatives. Due to nitro substituent in both compounds, it can be suggested that electron withdrawing group has very important contribution to enhance inhibition potency against hCA I. Furthermore, higher inhibition potencies of thiophene based compounds **3a**, **3c** and **3e** than those of furan bearing derivatives **3h**, **3i** and **3j** indicate that thiophene ring has more impact to enhance hCA I inhibition when compared with furan ring. When the CA II inhibition potentials of the compounds are examined, it is seen that the

Table 1
Human CA isoenzymes (*h*CA I and II) inhibition value of the compounds (**3a-3n**).

Compounds	IC_{50}(μM)				Ki(μM)	
	*h*CA I	r^2	*h*CA II	r^2	*h*CA I	*h*CA II
3a	0.732	0.9347	1.754	0.9668	0.3110 ± 0.103	1.3594 ± 0.354
3b	1.586	0.9512	1.378	0.9517	0.8190 ± 0.205	1.2442 ± 0.342
3c	0.692	0.9399	1.853	0.9903	0.3445 ± 0.112	1.0974 ± 0.259
3d	0.772	0.9568	1.893	0.9479	0.2653 ± 0.047	1.5036 ± 0.451
3e	0.176	0.9504	1.974	0.9637	0.1676 ± 0.017	1.5154 ± 0.375
3f	2.003	0.9505	1.634	0.9510	1.1014 ± 0.396	0.9596 ± 0.215
3g	1.627	0.9547	2.094	0.9825	1.1364 ± 0.238	1.2963 ± 0.357
3h	1.205	0.9856	2.044	0.9443	0.6454 ± 0.115	2.4180 ± 0.415
3i	1.963	0.9914	2.484	0.9809	1.7470 ± 0.355	2.4822 ± 0.490
3j	0.264	0.9445	2.415	0.9852	0.2383 ± 0.057	1.8232 ± 0.474
3k	1.098	0.9713	1.456	0.9561	2.0480 ± 0.314	1.6259 ± 0.408
3l	2.063	0.9716	1.791	0.9852	2.2538 ± 0.338	1.1614 ± 0.422
3m	1.462	0.9576	0.526	0.9430	1.8580 ± 0.409	0.2880 ± 0.080
3n	2.398	0.9643	0.637	0.9897	3.1280 ± 0.403	0.5722 ± 0.108
AZA	0.263	0.9567	0.108	0.9496	0.2892 ± 0.010	0.1355 ± 0.004

compounds **3m** and **3n** exhibit higher activity in the series. The compounds **3a-3l** include five membered thiophene, furan, pyyrole, or imidazole rings. On the other hand, there is a pyridine ring in the structure of compounds **3n** and **3m**. Thus, it can be proposed that unlike other compounds (**3a-3l**), the six-membered pyridine ring in the structures of **3n** and **3m** may be the reason for their higher activity.

The enzyme kinetic studies of all synthesized compounds **3a-3n** on both hCA I and hCA II enzymes were carried out in order to determine the inhibition type and calculate K_i values. The inhibition types are divided as reversible and irreversible inhibition. The uncompetitive, competitive, non-competitive and mixed type inhibitions constitute the subtypes of reversible inhibitors. All these subtypes of inhibition can be determined with the help of Lineweaver-Burk plots according to the style of graphics [51]. Uncompetitive type inhibition has parallel lines of inhibitor and control without any cross in the graphic. If there is an intersection in any area of the graph except for the x and y axes, the mixed type inhibition is concerned. The graph formed by the plots intersecting on y-axis describes the competitive inhibition type and this graphic has different slopes and intercepts on x-axis. Non-competitive inhibitors have the same intercept on x-axis and diverse slopes and intercepts on y-axis in the graphics. Lineweaver-Burk plots of the most active compounds **3e** and **3m** are presented in Figs. 2 and 3. Besides, Lineweaver-Burk plots of the other compounds are presented as supporting information (Supplementary Material Figs. S1–S26). These graphs intersect at the x-axis as in the non-competitive inhibition type described above. Hence, enzyme kinetic studies reveal that all synthesized compounds **3a-3n** are reversible and non-competitive inhibitors against hCA I and hCA II enzymes. K_i values were calculated by using the data gained from Lineweaver-Burk graphics. K_i values of the synthesized compounds were considered in the ranges of 0.1676–3.1280 μM and 0.2880–2.4822 μM on hCA I and hCA II, respectively. In addition to lowest IC_{50} compounds **3e** and **3m** also showed the lowest K_i values towards hCA I and hCA II enzyme (Table 1).

The K_i and IC_{50} of a drug to cause the inhibition of an enzyme is related to the concentration required to reduce the activity of this enzyme by half. More specifically, the K_i reflects the enzyme binding affinity of a drug, while the IC_{50} more exhibits the inhibitory potency of a drug on the enzyme. With lower K_i, the binding affinity required to inhibit the activity of the enzyme increases, while the amount of inhibitor decreases. Obtained results indicated that compounds **3e** and **3m** possess lower IC_{50} and K_i values against hCA I and hCA II than those of AZA. Besides, selectivity of compounds towards hCA I and hCA II are significantly different as seen in Table 1**.** These findings improve the biological importance of compounds **3e** and **3m** as selective inhibitors of hCA I and hCA II, respectively.

3.3. Cytotoxicity test

The simultaneous optimization of the desired drug properties and potential adverse effects are aimed in the early stages of new drug development studies. This approach allows scientists to select drug candidates with the highest probability of success for preclinical safety trials. Thus, some *in vitro* models are preferred for evaluating toxicity should be to predict human specific toxicity due to their high sensitivity in the determination of toxic agents [52]. In the present study MTT assay, a classical instance for such *in vitro* toxicity models, was performed using healthy NIH/3T3 mouse embryonic fibroblast cell lines (ATCC CRL1658), recommended cell type for general cytotoxicity screening by ISO (10993-5, 2009) [53]. As presented in the Table 2, the IC_{50} values of compounds **3e** and **3m** against NIH/3T3 cells were found to be higher than 1000 μM, which is significantly greater than the IC_{50} values of compounds against hCA I and II. Thus, it may be declared that both compounds are not toxic at their effective concentrations against hCA I and II.

3.4. Theoretical calculation of ADME parameters

Evaluation of the pharmacological properties of a drug candidate such as Absorption, Distribution, Metabolism and Excretion (ADME) has critical importance for initial selection. Thus, criteria for assessment of synthesized compounds during parent compound optimization can be established. Therefore, in the present study ADME properties were calculated using *QikProp 4.8*. [44] software and presented in the Table 3. *QikProp* also provides acceptable ranges for comparing the predicted properties of compounds with those of 95% of known drugs. Furthermore, the drug-likeness properties were estimated with the help of this software. The drug-likeness of all compounds was assessed according to Lipinski's Rule of Five [54] and Jorgensen's Rule of Three [55]. Lipinski's Rule of Five considers molecular weight (< 500 Da), number of hydrogen bond acceptors (≤10), number of hydrogen bond donors (≤5), and octanol/water partition coefficient (≤5), whereas Jorgensen's Rule of Three regards logS (> -5.7), PCaco (> 22 nm/s), primary metabolites (PM) (< 7). The violations of these rules are essential for the optimization of a biologically active compounds.

Table 3 contains the following parameters: Molecular weight (MW), number of rotatable bonds (RB), dipole moment (DM), molecular volume (MV), number of hydrogen donors (DHB), number of hydrogen acceptors (AHB), polar surface area (PSA), octanol/water partition coefficient (log P), aqueous solubility (log S), apparent Caco-2 cell permeability (PCaco), brain/blood partition coefficient (logBB), apparent MDCK cell permeability (PMDCK), number of likely primer metabolic reactions (PM), and percent of human oral absorption (% HOA), the violations of rules of three (VRT) and five (VRF). According

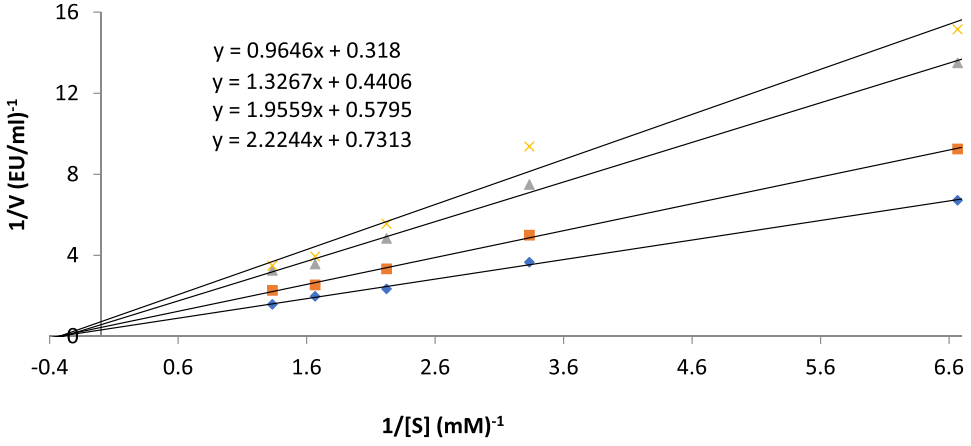

Fig. 2. Lineweaver–Burk graphs of the compound **3e** on CA I.

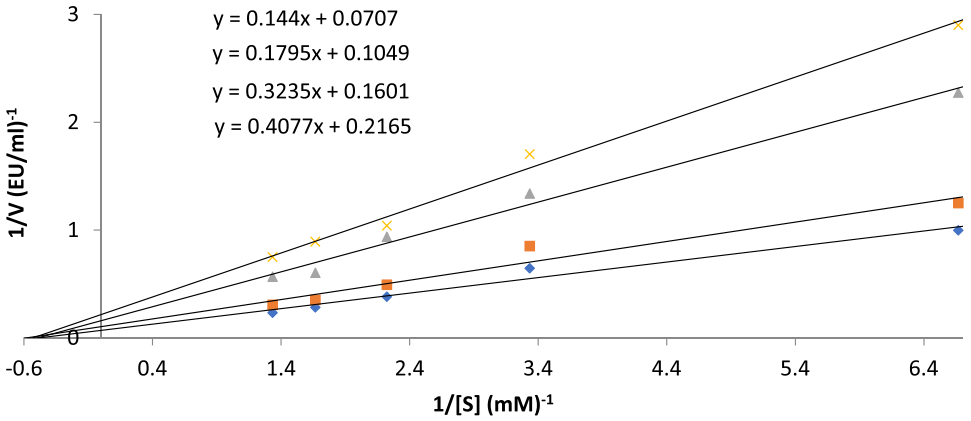

Fig. 3. Lineweaver–Burk graphs of the compound **3m** on CA II.

Table 2
IC_{50} (μM) values of the compounds **3a**, **3c**, **3d**, **3e**, **3j**, **3m** and **3n** derivatives against NIH/3T3 cell line.

Compound	3a	3c	3d	3e	3j	3m	3n
IC_{50} (μM)	> 1000	> 1000	> 1000	> 1000	> 1000	> 1000	> 1000

to Lipinski's rule of five and Jorgensen's rule of three all compounds **3a**-**3n** are in accordance with the rule by causing no more than one violation. Also, all ADME parameters of synthesized compounds **3a**-**3n** are in the recommended ranges. As a consequence of ADME predictions, it can be suggested that the final compounds **3a**-**3n** may have a good pharmacokinetic profile.

3.5. Molecular docking studies

The compounds **3e** and **3m** were found to be the most active derivatives against CAI and CA II enzymes as mentioned in the enzyme inhibition assay. Docking studies were performed in order to gain more insight into the binding modes of compounds **3e** and **3m** to evaluate the effects of structural modifications on the inhibitory activity against CAI and CA II. X-ray crystal structures of CA I (PDB ID: 1AZM) [45] and CA II (PDB ID: 3HS4) [46] were obtained from Protein Data Bank server

Table 3
Calculated ADME parameters.

Comp.	MW	RB	DM	MV	DHB	AHB	PSA	logP	logS	PCaco	logBB	PMDCK	PM	%HOA	VRF	VRT
3a	338.399	8	10.531	1029.269	4	9.5	126.840	0.55	−3.398	85.135	−2.130	61.661	3	64.709	0	0
3b	352.425	8	7.996	1053.538	4	9.5	120.894	0.797	−3.213	125.023	−1.776	96.890	4	69.145	0	0
3c	352.425	8	8.382	1073.871	4	9.5	123.862	0.77	−3.463	99.369	−1.983	68.771	4	67.198	0	0
3d	417.295	8	9.961	1083.843	4	9.5	126.824	1.081	−4.170	85.246	−2.005	161.973	3	67.830	0	0
3e	383.396	9	10.175	1099.002	4	10.5	173.861	−0.201	−3.276	9.439	−3.202	5.214	3	43.218	0	1
3f	321.353	8	9.341	1008.847	5	9.5	140.313	−0.031	−3.037	49.625	−2.495	19.577	2	57.115	0	0
3g	335.380	8	8.977	1047.045	4	9.5	126.734	0.524	−2.997	95.728	−2.027	39.826	2	65.473	0	0
3h	322.338	8	10.422	993.846	4	10	135.655	−0.018	−2.848	71.020	−2.295	28.841	3	59.974	0	0
3i	336.365	8	8.443	1041.415	4	10	132.802	0.273	−2.977	96.424	−2.079	40.139	4	64.058	0	0
3j	367.336	9	9.888	1071.889	4	11	183.310	−0.717	−2.880	7.759	−3.401	2.635	3	25.715	1	1
3k	322.341	8	9.528	984.063	5	11	151.938	−0.807	−2.519	32.237	−2.589	12.281	2	49.215	0	0
3l	336.368	8	10.156	1036.825	4	11	140.156	−0.248	−2.662	56.374	−2.274	22.470	2	56.834	0	0
3m	333.364	8	10.786	1031.598	4	11	136.385	−0.222	−2.747	54.918	−2.354	21.843	4	56.782	0	0
3n	333.364	8	10.245	1044.408	4	11	139.254	−0.198	−2.993	49.299	−2.514	19.438	4	56.087	0	0

MW: Molecular weight.
RB: Number of rotatable bonds.
DM: Computed dipole moment.
MV: Total solvent-accessible volume.
DHB: Estimated number of hydrogen bond donors.
AHB: Estimated number of hydrogen bond acceptors.
PSA: Van der Waals surface area of polar nitrogen and oxygen atoms and carbonyl carbon atoms.
logP: Predicted octanol/water partition coefficient.
logS: Predicted aqueous solubility.
PCaco: Predicted apparent Caco-2 cell permeability.
logBB: Predicted brain/blood partition coefficient.
PMDCK: Predicted apparent MDCK cell permeability.
PM: Number of likely metabolic reactions.
%HOA: Predicted human oral absorption percent.
VRF: Number of violations of Lipinski's rule of five. The rules are: MW < 500, logP < 5, DHB ≤ 5, AHB ≤ 10, Positive PSA value.
VRT: Number of violations of Jorgensen's rule of three. The three rules are: logS > −5.7, PCaco > 22 nm/s, PM < 7.

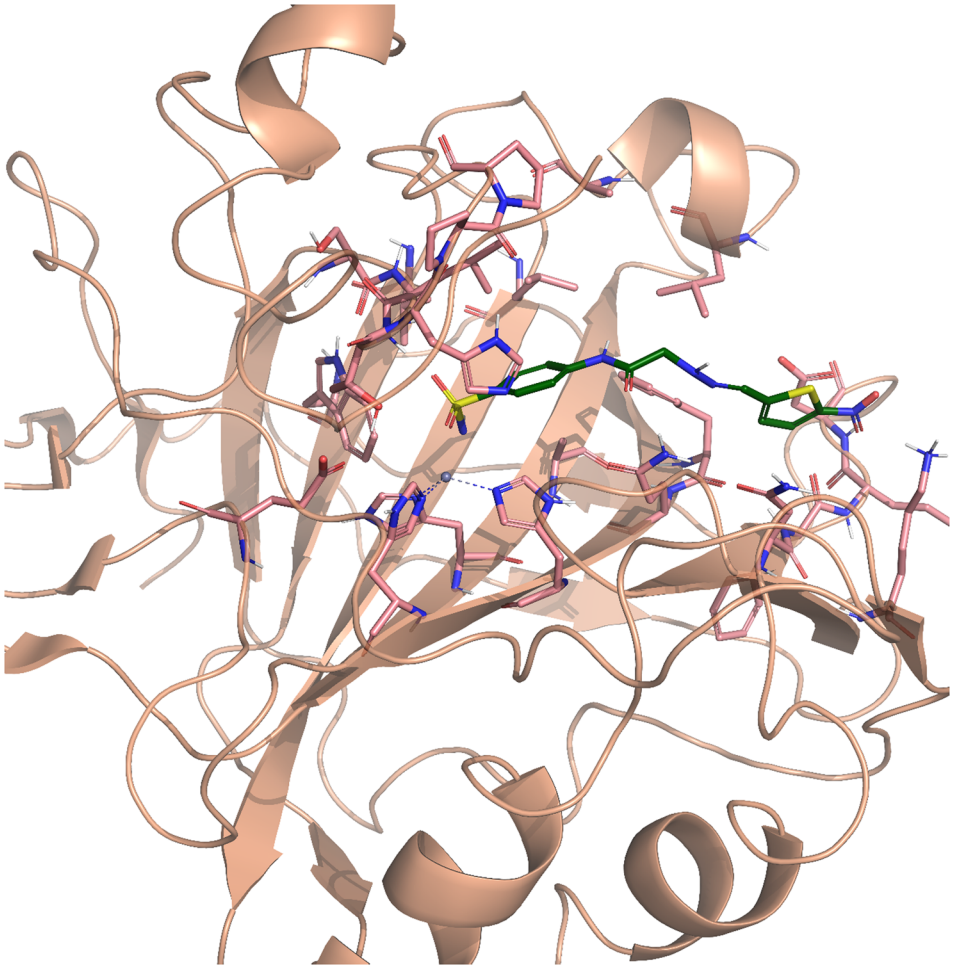

Fig. 4. Three-dimensional mode of compound **3e** in the enzyme active site of CA I (CA I PDB Code: 1AZM).

(www.pdb.org). The docking poses of compounds **3e** and **3m** are presented in Figs. 4, 5 and Supplementary Material Figs. S27–S36.

In the Supplementary Material Figs. S27 and S32, it can be seen that sulfonamide groups of compounds **3e** and **3m** are in N-deprotonated form, which serves as a zinc-binding site [56]. As expected, compounds **3e** and **3m** bind to enzyme active site by their sulfonamide groups coordinated to the zinc ion (Supplementary Material Figs. S28, S29, S33 and S34). The deprotonated sulfonamide amino groups bind to the Zn^{+2} ion by salt bridge. Also, one of oxygen atom of deprotonated sulfonamide group forms a metal coordination bond with Zn^{+2} ion. The other oxygen atom of deprotonated sulfonamide group creates a hydrogen bond with amino of Thr199 for compounds **3e** and **3m**. Both these interactions are typical for all sulfonamide-CA complexes investigated so far [56–62].

When docking poses of compound **3e** on CA I (Fig. 4 and Supplementary Material Figs. S27–S31) were analyzed, it can be seen that this compound has three interactions with enzyme active region, consist of a hydrogen bond, a π-π interaction and a salt bridge, except for mentioned above related to zinc ion. The hydrogen bond is seen between carbonyl of the structure and amino of Gln92. The phenyl ring in the structure is in an interaction with imidazole ring of Hid200 by doing π-π interaction. Furthermore, oxygen atom of nitro group is essential for strengthening binding to enzyme active site. This oxygen atom forms a salt bridge with quaternized amino of Lys57. Also, it can be seen from Supplementary Material Figs. S30 and S31 that van der Waals and electrostatic interactions provide stronger binding to enzyme active site of CA I for compound **3e**. This compound has favourable van der Waals interactions with Asn69, Hid67, Phe91, Gln92, Hid94, Hid96, Hid119, Ala121, Leu131, Leu141, Leu198, Thr199, Hid200 and Trp209, displayed with pink and red colours as described in the user guide of Glide [50]. Especially, it is thought that thiophene ring, hydrazine and amide moieties enhance van der Waals interaction with enzyme active region. Also, this compound shows promising electrostatic contributions with Hid94, Hid96, Glu106 and Hid119.

As mentioned in the enzyme inhibition assay, compound **3e** is the most active derivative against CA I with an IC_{50} value of 0.176 μM, while **3j** is the second active compound with an IC_{50} value of 0.264 μM. The structurally common feature of these compounds is the nitro group at C-5 position of both thiophene and furan rings. In this context, the docking studies supports the enzyme inhibition results. It is thought that the interactions related to nitro group at C-5 position of thiophene or furan is important in terms of explaining their inhibitory activities. It is seen that the presence of an electron withdrawing group such as nitro at this position is a positive contribution to the activity.

According to the docking poses of compound **3m** on CA II enzyme (Fig. 5 and Supplementary Material Figs. S32–S36), there are three hydrogen bonds apart from sulfonamide group interactions. The carbonyl of amide moiety of compound **3m** forms two hydrogen bonds with amino of Asn62 and Asn67. The nitrogen atom of pyridine ring in the structure has an additional interaction different from the interactions of the common chemical structure. This nitrogen atom is in interaction with nitrogen atom of indole ring of Trp5 by forming a hydrogen bond. Besides, van der Waals and electrostatic interactions of compound **3m** are presented in Supplementary Material Figs. S35 and S36. It can be seen that piperidine ring, hydrazine and amide moieties support binding to residues of enzyme active region of CA II by van der

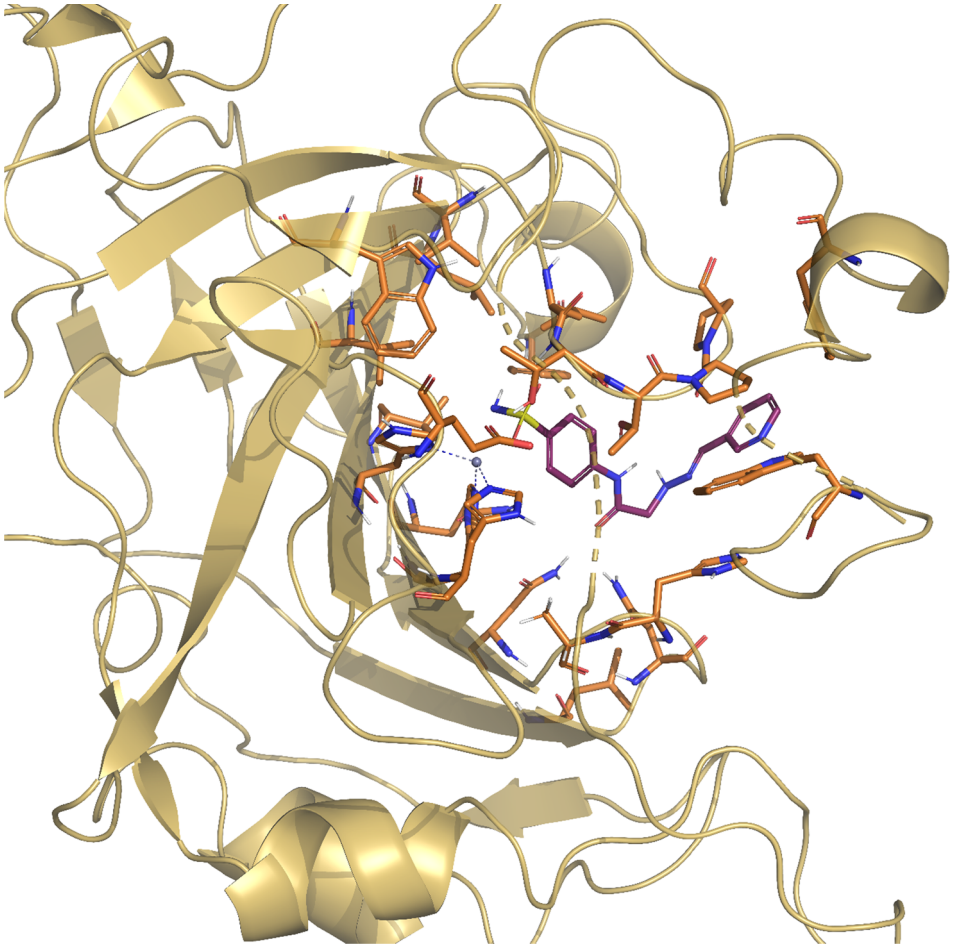

Fig. 5. Three-dimensional mode of compound **3m** in the enzyme active site of CA II (CA II PDB Code: 3HS4).

Waals interactions. This compound forms van der Waals interactions with Trp5, Asn62, Hid64, Gln92, Hid94, Hid96, Hid119, Val121, Val143, Leu198, Thr199, Thr200, Pro201, Pro202 and Trp209, which were shown as pink and red colours [50]. Electrostatic interactions between this compound and Hid96, Glu106 and Hid119 are also observed.

As stated in the enzyme activity results, compounds **3m** and **3n** are the most active derivatives against CA II enzyme with IC_{50} values of 0.526 and 0.637 μM, respectively. These compounds bear pyridine-3-yl and -4-yl rings different from common chemical structure. Docking studies provide to explain their inhibitory activities. The nitrogen atoms of pyridine rings have ability to form a hydrogen bond by acting as a hydrogen acceptor because their lone pair is ready for donation. Thus, pyridine nitrogen can interact with donor sites of amino acid residues in an enzyme active site. Consequently, this difference influences and explains binding capability of the compounds **3m** and **3n** to enzyme active site and enzyme inhibition potency.

4. Conclusion

In conclusion, we have reported the synthesis, characterization and evaluation of biological activity of a series of sulfonamide bearing hydrazone compounds for the inhibition of the physiologically relevant CA isozymes. According to Ki values, nitrothiophen compound **3e** toward hCA I and pyridin-3-yl compound **3m** toward hCA II can be considered as leader compounds for further studies. Enzyme inhibition is a very important issue for drug design and biochemical applications. Hence, the results put forward that new sulfonamide derivatives inhibit the hCA I and II enzyme activity, which will probably be enhanced in the further studies.

Acknowledgment

This study was financially supported by Anadolu University Scientific Projects Fund, Project No: 1803S050.

Declaration of interest

The authors declare no conflicts of interest.

Appendix A. Supplementary material

Supplementary data to this article can be found online at https://doi.org/10.1016/j.bioorg.2019.103153.

References

[1] H.I. Gul, E. Mete, P. Taslimi, I. Gulçin, C.T. Supuran, J. Enzyme Inhib. Med. Chem. 32 (2017) 189–192.
[2] M. D'Ascenzio, P. Guglielmi, S. Carradori, D. Secci, R. Florio, A. Mollica, M. Ceruso, A. Akdemir, A.P. Sobolev, C.T. Supuran, J. Enzyme Inhib. Med. Chem. 32 (2017) 51–59.
[3] S. Akocak, N. Lolak, A. Nocentini, G. Karakoc, A. Tufan, C.T. Supuran, Bioorg. Med. Chem. 25 (2017) 3093–3097.
[4] E. Dilek, H.S. Erol, A. Cakir, M. Koç, M.B. Halici, Arch. Physiol. Biochem. 123 (2017) 219–224.
[5] T. Gokcen, I. Gulcin, T. Ozturk, A.C. Goren, J. Enzyme Inhib. Med. Chem. 31 (2016) 180–188.
[6] D.A. Ibrahim, D.S. Lasheen, M.Y. Zaky, A.W. Ibrahim, D. Vullo, M. Ceruso, C.T. Supuran, D.A.A. El Ella, Bioorg. Med. Chem. 23 (2015) 4989–4999.
[7] M. Aggarwal, C.D. Boone, B. Kondeti, R. McKenna, J. Enzyme Inhib. Med. Chem. 28

(2) (2013) 267–277.
[8] C.T. Supuran, Curr. Pharm. Des. 14 (2008) 603–614.
[9] B.C. ripp, K. Smith, J.G. Ferry, J. Biol. Chem. 276 (52) (2001) 48615–48618.
[10] D. Vullo, M. Franchi, E. Gallori, J. Antel, A. Scozzafava, C.T. Supuran, J. Med. Chem. 47 (2004) 1272–1279.
[11] I. Nishimori, D. Vullo, A. Innocenti, A. Scozzafava, A. Mastrolorenzo, C.T. Supuran, J. Med. Chem. 48 (2005) 7860–7866.
[12] I. Nishimori, T. Minakuchi, S. Onishi, D. Vullo, A. Scozzafava, C.T. Supuran, J. Med. Chem. 50 (2007) 381–388.
[13] D. Vullo, M. Franchi, E. Gallori, J. Pastorek, A. Scozzafava, S. Pastorekova, Bioorg. Med. Chem. Lett. 13 (2003) 1005–1009.
[14] J.J. Baldwin, G.S. Ponticello, P.S. Anderson, M.E. Christy, M.A. Murcko, W.C. Randall, H. Schwam, M.F. Sugrue, J.P. Springer, P. Gautheron, J. Grove, P. Mallorga, M.P. Viader, B.M. McKeever, M.A. Navia, J. Med. Chem. 32 (12) (1989) 2510–2513.
[15] C.T. Supuran, A. Di Fiore, G. De Simone, Expert Opin. Emerg. Drugs 13 (2) (2008) 383–392.
[16] S. Carradori, A. Mollica, C. De Monte, A. Ganese, C.T. Supuran, Molecules 20 (4) (2015) 5667–5679.
[17] D. Vullo, M. Franchi, E. Gallori, J. Pastorek, A. Scozzafava, S. Pastorekova, C.T. Supuran, Bioorg. Med. Chem. Lett. 13 (6) (2005) 1005–1009.
[18] C.T. Supuran, Nat. Rev. Drug Discov. 7 (2) (2008) 168–181.
[19] A. Thiry, J.M. Dogné, C.T. Supuran, B. Masereel, Curr. Pharm. Des. 14 (7) (2008) 661–671.
[20] F. Carta, C.T. Supuran, Expert Opin. Ther. Pat. 23 (6) (2013) 681–691.
[21] H. Tanimukai, M. Inui, S. Hariguchi, Z. Kaneko, Biochem. Pharmacol. 14 (6) (1965) 961–970.
[22] E. Masini, F. Carta, A. Scozzafava, C.T. Supuran, Expert Opin. Ther. Pat. 23 (6) (2013) 705–716.
[23] N. Büyükkıdan, B. Büyükkıdan, M. Bülbül, R. Kasımoğulları, S. Mert, J. Enzyme Inhib. Med. Chem. 32 (2017) 208–213.
[24] E. Bruno, M.R. Buemi, A. Di Fiore, L. De Lua, S. Ferro, A. Angeli, R. Cirilli, D. Sadutto, V. Alterio, S.M. Monti, C.T. Supuran, G. De Simone, R. Gitto, J. Med. Chem. 60 (2017) 4316–4326.
[25] M. Bozdag, A.M. Alafeefy, A.M. Altamimi, F. Carta, C.T. Supuran, D. Vullo, Bioorg. Med. Chem. 25 (2017) 2782–2788.
[26] F.R. Li, Z.F. Fan, S.J. Qi, Y.S. Wang, J. Wang, Y. Liu, M.S. Cheng, Molecules 22 (2017) 785.
[27] E.R. Swenson, Expert Opin. Drug Saf. 13 (2014) 459–472.
[28] E. Başar, E. Tunca, M. Bülbül, M. Kaya, J. Enzyme Inhib. Med. Chem. 31 (2016) 1356–1361.
[29] H.I. Gul, E. Mete, E. Eren, H. Sakagami, C. Yamali, C.T. Supuran, J. Enzyme Inhib. Med. Chem. 32 (2017) 169–175.
[30] A.M. Alafeefy, H.A. Abdel-Aziz, D. Vullo, A.M.S. Tamami, A.S. Awaad, M.A. Mohamed, C. Capasso, C.T. Supuran, J. Enzyme Inhib. Med. Chem. 30 (2015) 52–56.
[31] M. Durgun, H. Turkmen, M. Ceruso, C.T. Supuran, Bioorg. Med. Chem. Lett. 25 (2015) 2377–2381.
[32] M.S. Alam, D.U. Lee, Arch. Pharm. Res. 39 (2016) 191–201.
[33] F. Hamurcu, S. Mamaş, U.O. Ozdemir, A.B. Gündüzalp, O.S. Sentürk, J. Mol. Struct. 1118 (2016) 18–27.
[34] Z.H. Li, D.X. Yang, P.F. Geng, J. Zhang, H.M. Wei, B. Hu, Q. Guo, X.H. Zhang, W.G. Gou, B. Zhao, B. Yu, L.Y. Ma, H.M. Liu, Eur. J. Med. Chem. 124 (2016) 967–980.
[35] P. Nagender, R.N. Kumar, G.M. Reddy, D.K. Swaroop, Y. Poornachandra, C.G. Kumar, B. Narsaiah, Bioorg. Med. Chem. Lett. 26 (2016) 4427–4432.
[36] M.D. Altıntop, B. Sever, A. Özdemir, K. Kucukoğlu, H. Onem, H. Nadaroglu, Z.A. Kaplancıklı, Bioorg. Med. Chem. 25 (2017) 3547–3554.
[37] S. Iqbal, M. Saleem, M.K. Azim, M. Taha, U. Salar, K.M. Khan, S. Perveen, M.I. Choudhary, Bioorg. Chem. 72 (2017) 89–101.
[38] K. Kucukoglua, H.I. Gul, P. Taslimi, I. Gulcin, C.T. Supuran, Bioorg. Chem. 86 (2019) 316–321.
[39] S. Mert, Z. Alım, M.M. İşgör, B. Anıl, R. Kasımoğulları, Ş. Beydemir, Arab. J. Chem. (2015).
[40] K.M. Wilbur, N.G. Anderson, J. Biol. Chem. 176 (1948) 147–154.
[41] J.A. Verpoorte, S. Mehta, J.T. Edsall, J. Biol. Chem. 42 (1967) 4221–4229.
[42] Ü.D. Özkay, Ö.D. Can, B.N. Saglık, U.A. Cevik, S. Levent, Y. Özkay, S. Ilgın, Ö. Atlı, Bioorg. Med. Chem. Lett. 26 (2016) 387–5394.
[43] B.N. Sağlık, S. Ilgın, Y. Özkay, Eur. J. Med. Chem. 124 (2016) 1026–1040.
[44] QikProp, version 4.8, Schrödinger, LLC, New York, NY, 2016.
[45] S. Chakravarty, K.K. Kannan, J. Mol. Biol. 243 (1994) 298–309.
[46] K.H. Sippel, A.H. Robbins, J. Domsic, C. Genis, M. Agbandje-McKenna, R. McKenna, Acta Crystallogr, Sect. F. Struct. Biol. Cryst. Commun. 65 (2009) 992–995.
[47] Maestro, version 10.6, Schrödinger, LLC, New York, NY, 2016.
[48] Schrödinger, LLC, New York, NY, 2016.
[49] LigPrep, version 3.8, Schrödinger, LLC, New York, NY, 2016.
[50] Glide, version 7.1, Schrödinger, LLC, New York, NY, 2016.
[51] N.V. Bhagavan, 1st ed. Elsevier, Burlington, MA, USA, 2011, p. 47–58.
[52] J.M. McKim Jr., Comb. Chem. High Throughput. Screen. 13 (2010) 188–206.
[53] International Organization for Standardization, Biological Evaluation of Medical Devices-part 5: Tests for in vitro Cytotoxicity ISO-10993-5, third ed., 2009.
[54] C.A. Lipinski, F. Lombardo, B.W. Dominy, P.J. Feeney, Adv. Drug Deliv. Rev. 46 (2001) 3–26.
[55] W.L. Jorgensen, E.M. Duffy, Adv. Drug Deliv. Rev. 54 (2002) 355–366.
[56] R.W. King, A.S. Burgen, Biochim. Biophys. Acta 207 (1970) 278–285.
[57] F. Abbate, C.T. Supuran, A. Scozzafava, P. Orioli, M.T. Stubbs, G. Klebe, J. Med. Chem. 45 (2002) 3583–3587.
[58] F. Pacchiano, F. Carta, P.C. McDonald, Y. Lou, D. Vullo, A. Scozzafava, S. Dedhar, V.T. Supuran, J. Med. Chem. 54 (2011) 1896–1902.
[59] J. Ivanova, A. Balode, R. Žalubovskis, J. Leitans, A. Kazaks, D. Vullo, K. Tars, C.T. Supuran, Bioorg. Med. Chem. 25 (2017) 857–863.
[60] J. Leitans, A. Sprudza, M. Tanc, I. Vozny, R. Zalubovskis, K. Tars, C.T. Supuran, Bioorg. Med. Chem. 21 (2013) 5130–5138.
[61] B.S. Avvaru, J.M. Wagner, A. Maresca, A. Scozzafava, A.H. Robbins, C.T. Supuran, R. McKenna, Bioorg. Med. Chem. Lett. 20 (2010) 4376–4381.
[62] J. Ivanova, J. Leitans, M. Tanc, A. Kazaks, R. Zalubovsis, C.T. Supuran, K. Tars, Chem. Commun (Camb) 51 (2015) 7108–7111.